A Unified Mechanistic Concept of the Copper-Catalyzed and Amide-Oxazoline Directed C(sp^2)–H Bond Functionalization

Li-Ping Xu,[1,3] Brandon E. Haines,[1] Manjaly J. Ajitha,[1] Jin-Quan Yu,[2] and Djamaladdin G. Musaev*,[1]

[1] Cherry L. Emerson Center for Scientific Computation, and Department of Chemistry, Emory University, 1521 Dickey Drive, Atlanta, Georgia, 30322, United States;

[2] Department of Chemistry, The Scripps Research Institute, 10550 North Torrey Pines Road, La Jolla, California, 92037, United States;

[3] School of Chemistry and Chemical Engineering, Shandong University of Technology, Zibo, 255000, China.

ABSTRACT: Density functional theory (DFT) calculations have been performed to provide the unified mechanism of the Cu(II)-catalyzed and amide-oxazoline (Oxa) directed C(sp^2)–H functionalization reactions. The common steps of the studied seven reactions (such as C–H bond vinylation, phenylation, trifluoromethylation, amination, alkynylation, and hydroxylation) are the complexation, N–H and C–H bond deprotonation, and Cu(II)/Cu(II) → Cu(I)/Cu(III) disproportionation steps, leading to the Cu(III)-intermediate. The mechanism of the studied C–H functionalization reactions, initiated from the Cu(III)-intermediate, depends on the nature of coupling partners. With vinyl- or phenyl-Bpin, which bear no acidic proton (called as a Type–I reaction), the coupling partners are the *in situ* generated (by addition of anions) anionic borates, which coordinate to the Cu(III)-intermediate and undergo concerted transmetalation and reductive elimination to form a new C-C bond. In contrast, with imidazole, aromatic amines, terminal alkyne, and water (called as a Type–II reaction), which bear an acidic proton, a real coupling partners are their *in situ* generated deprotonated derivatives, which coordinate to copper and lead to final product with the C–Y bond (Y = C, N, O) via the reductive elimination pathway. The C(sp^2)–H bond trifluoromethylation with $TMSCF_3$ is identified as a special case, positioned between the Type–I and Type–II reaction types. The real coupling partner of this reaction is the *in situ* generated (via the CF_3^--to-OH^- ligand exchange) CF_3^- anion that binds to the Cu(III)-intermediate and undergoes the C–CF_3 reductive elimination. Our calculations, consistent with the experimental KIE study, which have established the C–H bond activation as a rate-limiting step for all reactions.

Keywords: Cu-catalyst, CH functionalization, Directing group assisted**,** Reaction Mechanism, DFT calculations

Introduction

The transition-metal-catalyzed C–H functionalization is established as an elegant, step- and atom-economic methodology of organic synthesis.[1-8] However, majority of these reactions use the expensive noble transition metals such as Pd, Rh, and Ru, which limits their industrial applications. Therefore, the development of the C–H functionalization methodology involving earth-abundant first-row transition metals[9] (such as iron,[10,11] cobalt,[12,13] nickel,[14-16] and copper[17-19]), as well as catalysis with noble metals but with millions turnover numbers (TON) have established as one of the major research direction.[20-22] Among the emerging directions, the copper-catalyzed selective C–H bond functionalization in various biologically and chemically accessible small molecules has attracted significant interest.[23-25]

As example, Yu and coworkers have recently established the copper-catalyzed and amide-oxazoline (Oxa) ligand directed C(sp^2)–H functionalization. [25-31] They have reported the C(sp^2)–H (a) vinylation (Scheme 1, eq. 1)[25] and phenylation (Scheme 1, eq. 2)[26] with vinyl and phenyl boronic ester (R–Bpin), (b) trifluoromethylation[27] with $TMSCF_3$ (Scheme 1, eq. 3), (c) amination with azaheterocycles (Scheme 1, eq. 4)[28] or aromatic (Scheme 1, eq. 5)[29] amines, (d) alkynylation[30] with aryl or alkyl-substituted terminal alkyne (Scheme 1, eq. 6), and (e) hydroxylation[31] with water (Scheme 1, eq. 7). While this novel strategy has opened new horizons for selective transformation of the C(sp^2)–H bond into the C–C, C–N, and C–O bonds using inexpensive copper catalysts and broadly available reaction coupling partners, the lack of atomistic level understanding of the mechanisms and controlling factors of these reactions limits extension of their substrate scope and broader applications. Unfortunately, the acquiring of such detailed fundamental knowledge still is challenging and remains highly underdeveloped compared to the C–H functionalization reactions catalyzed by second-row transition metal catalysts, for example Pd.[32-42] There are several issues which limits such mechanistic studies of the Cu-catalyzed C–H functionalization.

One of them is an easy accessibility of the 0, +1, +2, and +3 oxidation states of Cu-complexes.[43,44] This feature of copper enables the Cu-complexes act as a both one-electron (i.e., to promote the radical reactions) and two-electron (i.e., to promote the organometallic pathways) redox catalyst,[9] and the Cu-catalyzed C(sp^2)–H functionalization proceeds via the Cu(I)/Cu(III),[45,46] Cu(0)/Cu(II),[47-49] or Cu(I)/Cu(II)[46,50] catalytic cycles.

Scheme 1. Selected Example for Cu-Mediated/Catalyzed C(sp²) − H Functionalization.

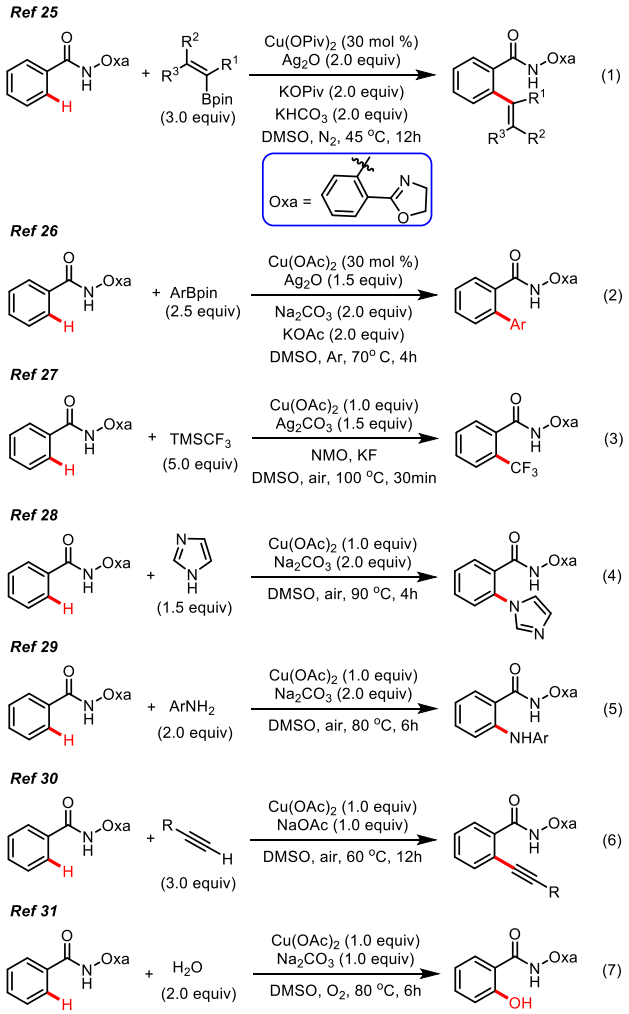

For instance, Yu and coworkers, in their Cu(II)-catalyzed aryl C–H bond functionalization using O_2 as an oxidant, have proposed a single-electron-transfer (SET) mechanism (i.e., Cu(I)/Cu(II) cycle, Scheme 2, eq. 8).[23] Stahl, Cramer and coworkers, in their experimental and computational studies of the Cu-mediated oxidation of *N*-(8-quinolinyl)benzamide, have shown that the mechanism of the Cu-catalyzed C–H functionalization could be even more complex and depends on the reaction conditions (Scheme 2, eq. 9).[50] They have established that under basic condition, the directed C–H methoxylation or chlorination of benzamide occurs via the organometallic (i.e., Cu(I)/Cu(III) cycle) pathway, while it proceeds through an SET mechanism (i.e., Cu(I)/Cu(II) cycle) for nondirected chlorination of quinoline under acidic condition.[50] Recently, Wang, Wu, Zhang and coworkers have reported a detailed mechanistic study[51] on the Cu(II)-catalyzed cross-coupling between azacalix[1]arene[3]pyridine and arylboronic acid[52-56] (Scheme 2, eq. 10), and proposed the Cu(II)/Cu(III) catalytic cycle for this reaction.

Another degree of complexity to the Cu-catalyzed and directing group mediated C–H functionalization, comes from the comparability of redox potentials of Cu and some of the extensively utilized auxiliary ligands (i.e., redox non-innocent ligands). We should emphasize that this phenomenon opens new directions (i.e., ligand enabled) in designing of the Cu-catalyzed C–H functionalization.[9,57-58]

We also wish to mention the chameleon nature of aggregation stages of the catalytic active species in course of the Cu-catalyzed chemical transformations. Today, in majority of reported mechanistic analyses for the homogenous Cu-catalyzed C–H functionalization reactions, the active catalyst is assumed to be the mono-copper complexes. However, existing literature, as well as our own studies, indicate the possibility of involvement of various dimers (depending on the reaction conditions) or/and higher order nano-clusters of Cu, to the Cu-catalyzed organic transformations.[59,60] As example, recently, Musaev, Itami and coworkers have demonstrated that catalytic active species in the CuX-complexes (where X = Cl, Br, or I) catalyzed aromatic C–H bond imidation with *N*-fluorobenzenesulfonimide (NFSI) as an oxidant is a *bis*-fluoro-dinuclear Cu^{II}/Cu^{II} species.[19]

Scheme 2. Selected Mechanistic Studies on Cu(II)-Catalyzed/Mediated C(sp²) − H Functionalization.

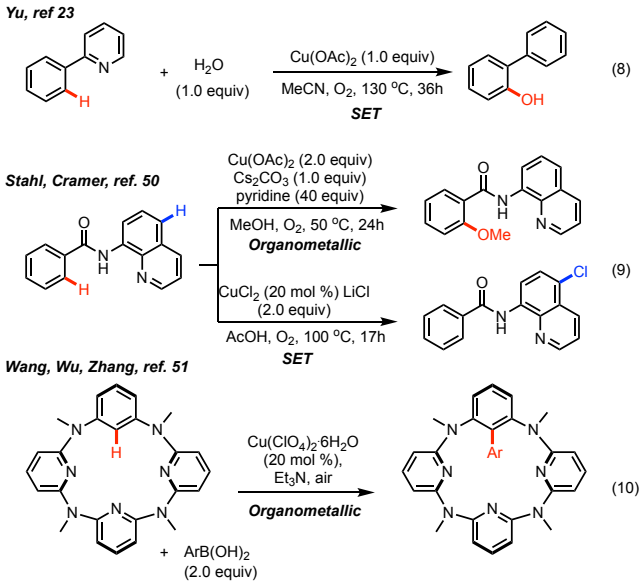

With these challenges in mind, we launched in-depth computational analyses of the reactions presented in Scheme 1. Our major goals are to: (a) provide a unified mechanistic view to the Cu(II)-catalyzed and amide-oxazoline (Oxa) directed C(sp²)–H functionalization strategy, developed by Yu and coworkers,[25-31] and (b) identify critical factors (such as the role of base, coupling partner, electronic features of the utilized substrates, etc.) on the success of these reactions. We are confident that such a comprehensive and atomistic-level mechanistic approach will enable chemists to design more effective Cu(II)-catalyzed C(sp²)–H bond functionalization reactions assisted by the weakly coordinated ligands.

To initiate our studies, we summarize the previously proposed Cu(II)-catalyzed and amide-oxazoline directed C(sp²)–H functionalization (Scheme 3).[25,31] In general, initial common steps of these reactions are proposed to be: (a) the substrate coordination (by its directing group, DG) to the Cu-center,

followed by the N–H and C–H bond activation to form intermediate **B**, and (b) the Cu(II)/Cu(II)–to– Cu(I)/Cu(III) disproportionation to form the Cu(III) intermediate **C**. With coupling partners like R–Bpin, the following steps are (c) transmetalation leading to intermediate **D**, (d) reductive elimination to form **E**, and (e) protodemetalation (i.e., formation of **F**) and catalyst regeneration (i.e. Cu(I)→Cu(II) oxidation).[25] Alternatively, a direct reductive elimination from **C** to form intermediate **H** and the following hydrolysis with H_2O would lead to the hydroxylation product.[31]

Scheme 3. Previously Proposed Catalytic Cycle for the Cu(II)-Catalyzed and Amide-Oxazoline (Oxa) Directed (DG) C(sp²)–H Bond Functionalization. Reproduced from Refs. 25 and 31, Copyright [years of 2015 and 2020] American Chemical Society.

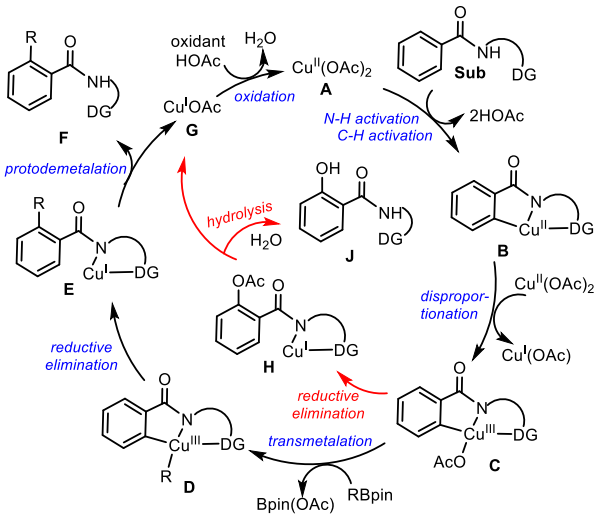

Computational Details

Geometry and frequency calculations for all reported structures were performed with the Gaussian09 suite of programs[61] at the [B3LYP-D3]/[6-31G(d,p) + Lanl2dz (Cu,Cs)] level of theory with the corresponding Hay-Wadt effective core potential[62,63] for Cu and Cs. Thus, here we used the B3LYP[64-65] density functional with Grimme's empirical dispersion-correction (D3).[67,68] This method is shown to be reliable for the Cu-catalyzed organometallic system in previous studies.[19,51] The performed frequency calculations enabled to confirm the stationary points as minima (with zero imaginary frequency) or transition state (with one imaginary frequency), and to calculate thermal and entropy corrections to the energies. Intrinsic reaction coordinate (IRC) calculations were performed for selected transition states to ensure their true nature and connect them with proper reactants and products. Bulk solvent effects were incorporated in all calculations with the experimentally[25-31] used DMSO as the solvent (including the geometry optimization and frequency calculations) at the self-consistent reaction field polarizable continuum model (IEF-PCM)[69] level of theory.

In the presented studies of the reactions (1-7), we used benzamide-oxazoline, BAO, as a substrate, in conjunction with the experimentally utilized coupling partners. As a catalyst, we choose the "add-in" $Cu(OAc)_2$ (**1**) complex, while our calculations show that the dimerization of $Cu(OAc)_2$ to give $Cu_2(OAc)_4$ is 18.2 kcal/mol exergonic (see Scheme S1 in the Supporting Information). Here, we hypothesize that under the reaction conditions, the $Cu_2(OAc)_4 \leftrightarrow 2\ Cu(OAc)_2$ equilibrium is reachable. Furthermore, the use of $Cu(OAc)_2$ monomer as a catalyst will empower us for better understanding of mechanism and intrinsic controlling factors of the Cu(II)-catalyzed C(sp²)–H functionalization.

Here, we calculated and analyzed several low-lying electronic states (including the ferromagnetically coupled (i.e. open-shell) singlet states) of every reported intermediate and transition state, while, below, only their energetically lowest electronic states will be discussed. In our discussion, the energies are presented as ΔG(ΔH), in kcal/mol, unless otherwise stated. Calculated cartesian coordinates and energies of all reported species are provided in the Supporting Information.

To elucidate impact of the used computational approach to the below reported major conclusions, we also performed the single point energy calculations by using the triple-zeta basis sets {[6-311++G(d,p)] for C, H, O, and N atoms, and SDD basis set for Cu atom} for all reported structures of the key reaction pathways. In general, we found that the use of the high-level basis sets, did not change the reported trends and major conclusions. Therefore, below we discuss only the results obtained at the double zeta basis set calculations (in sake of their completeness), but include the results of the high-level triple-zeta basis set calculations in the supporting information.

Results and Discussion

1. Initial Steps of the Studied Reactions.

As mentioned above, initial steps of the reactions (1-7) (see Scheme 1), i.e., (a) the substrate coordination (by its oxazoline directing group, DG) to the Cu-center, the N–H bond activation and following the C–H bond deprotonation to form intermediate **B**, and (b) the Cu(II)/Cu(II)–to–Cu(I)/Cu(III) disproportionation to form the Cu(III) intermediate **C** (see Scheme 3), are independent of the coupling partners of the reaction. Our calculations show that the coordination of substrate BAO to $Cu(OAc)_2$ (**1**) is result of the weak Cu–N interaction, and the N–H bond deprotonation requires only 7.4 kcal/mol free energy at the transition state **3-ts** to generate intermediate **4** with hydrogen bonding between the AcOH and the N-atom of the ligand (see Figure 1).[70] The dissociation of the generated AcOH and reorganization of **4** lead to intermediate **5**: as seen in Figure 1, the formation of **5** is 9.0 kcal/mol less favorable than starting species, i.e. $Cu(OAc)_2$ + BAO. In intermediate **5** the C–H activation occurs (via the CMD mechanism) through transition state **6-ts** and leads to the Cu(II)-intermediate **7**. As seen in Figure 1, the C–H activation in **5** requires 21.9 kcal/mol intrinsic activation barrier (relative to the pre-reaction complex **5**). The overall energy required for the redox neutral C–H bond activation is 30.9 kcal/mol, calculated from the reactants **1** + BAO. Furthermore, the formation of the product complex **7** is endergonic by 24.8 kcal/mol. The subsequent disproportionation by another Cu(II) species $Cu^{II}(OAc)_2$ generates Cu(I) species $[Cu^{I}(OAc)(HOAc)]$ and the concomitant Cu(III) intermediate, **8**. This disproportionation step, i.e. reaction **7** → **8**, is exergonic by 6.2 kcal/mol. Regardless, the product complex **8** is 18.6

kcal/mol higher in free energy than starting species, i.e. $2Cu(OAc)_2$ + BAO.

In the absence of coupling partner, intermediate **8** could be expected to undergo the C–O reductive elimination (i.e., acetoxylation). The presented calculations show that direct C–O bond formation in **8** requires a 36.5 kcal/mol free energy barrier, calculated relative to $2Cu(OAc)_2$ + BAO, at the transition state **9-ts**. This free energy barrier is higher than 30.9 kcal/mol for the C–H bond activation, indicating that the C–O reductive elimination is the rate-determining step of the acetoxylation reaction. Therefore, we conclude that the Cu(II)-catalyzed C(sp^2)–H bond acetoxylation in benzamide-oxazoline via the direct C–O reductive elimination from intermediate **8**, without coupling partner, is unlikely. This conclusion contrasts to previously proposed mechanistic scenario[31] (see red pathway in Scheme 3), and indicates that the Cu(II)-catalyzed C(sp^2)–H bond acetoxylation in BAO may occurs via different pathway than direct C-O reductive elimination from intermediate **8** with Cu(III)-center. Since the acetoxylation from **8**, in the absence of coupling partner, is not a subject of this paper, below we will not discuss this reaction further in detail.

In the presence of the coupling partners, the transformation of intermediate **8** to the final products, as it could be expected, is function of physicochemical properties of the used coupling partners and reaction conditions (including the nature of nucleophile, base, temperature, solvent, oxidant, and more).

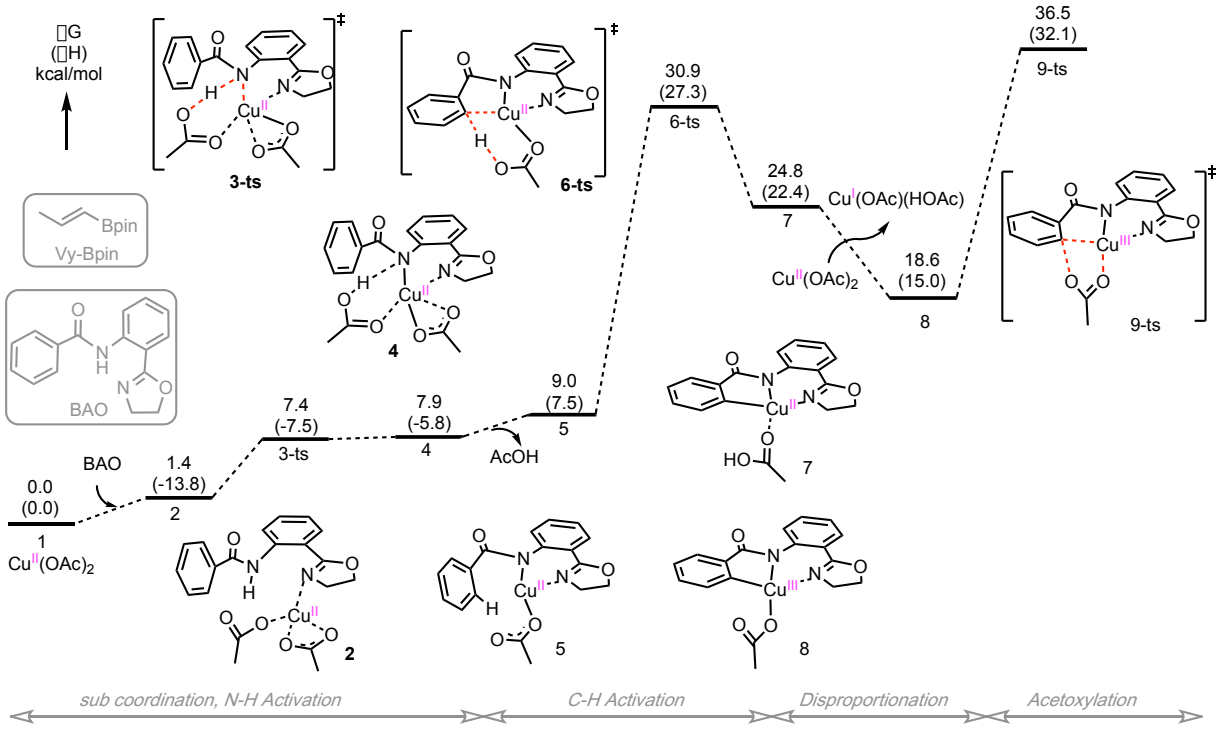

Figure 1. Potential energy surface for the initial steps of the studied reactions (1-7), namely, Substrate (BAO) coordination, N-H bond activation, C-H bond deprotonation, and Cu(II)/Cu(II) → Cu(I)/Cu(III) disproportionation steps, as well as the direct C–O bond formation in the resulted complex **8**.

To proceed our investigation on the mechanism of reactions (1-7) (Scheme 1), we divided them into two classes, based on the used coupling partners (see Table 1). Type-I reactions (1-2) are those with coupling partners bearing no acidic hydrogens (i.e., Ar–Bpin and vinyl–Bpin). The coupling partners of these reactions might be either charge neutral or anionic (formed by addition of base ion, for example as Ar–Bpin(X)$^-$ and vinyl–Bpin(X)$^-$, respectively, where X could be OH, OAc, and other anions) species generated under the reaction conditions. Type-II reactions (4-7) are those in which the coupling partners bear acidic hydrogens (such as imidazole, $ArNH_2$, terminal alkyne, and H_2O). We hypothesize that under the reaction condition these coupling partners can be in their either charge neutral or deprotonated forms (i.e., in their anionic forms, such as the imidazole anion, $ArNH^-$, RCC^-, and OH^-). Reaction (3) with $TMSCF_3$, while formally relates to the Type-I reactions, is a special case (see below).

Table 1. The Type-I and Type-II Classification of the Studied Reactions Based on the Participating Coupling Partners.

	Type-I, no acidic H	Type-II, with acidic H
Coupling Partners	Ar-Bpin Vinyl-Bpin $TMS-CF_3$	Terminal Alkyne $ArNH_2$ Imidazole H_2O

Main elementary reactions initiated from the previously generated intermediate **8** by adding the coupling partners can be the (a) complexation, (b) transmetalation, and (c) C–Y reductive elimination, which we analyze below for each reaction types.

2. Type–I Reactions

2.1. Transmetalation and Reductive Elimination

To demonstrate complexity of the mechanism and identify controlling factors of the Type-I reactions, we chose to report the BAO C(sp^2)–H bond vinylation by vinyl–Bpin, while we also have explored mechanism of the BAO C(sp^2)–H bond phenylation with phenyl boronic esters (see Figure S1 in the Supporting Information), the key results of which will be briefly summarized below. We initiated our investigations on the previously proposed reaction pathway, I-*path-a* (see Scheme 3 and Figure 2), that starts by the charge neutral vinyl–Bpin coordination to **8** with a weak Cu-vinyl interaction, and follows via the transmetalation and reductive elimination steps.[25,26] We found that the transmetalation step of this pathway requires a prohibitatively high free energy barrier of 46.4 kcal/mol (calculated relative to the reactants, 2 $Cu(OAc)_2$ + BAO + vinyl–Bpin). Therefore, we concluded that $Cu(OAc)_2$-catalyzed BAO C(sp^2)–H bond vinylation by the charge neutral vinyl–Bpin is unlikely to proceed. This finding is consistent with the available general knowledge that in the Pd-catalyzed cross coupling reactions with organoboron species (e.g., Suzuki reaction): the organoboronic acids/esters do not transmetalate to the Pd(II)-complexes.[71]

On the other hand, it is also well-established that the corresponding ate-complexes (borates), which can be formed by the addition of base anion to the boron center, may readily undergo transmetallation.[72] With this knowledge, we investigated the possibilities of the borate participation in the transmetalation in the $Cu(OAc)_2$ catalyzed BAO C(sp^2)–H bond vinylation. Here, for sake of simplicity, we chose the vinyl-Bpin(OH)$^-$ anion as a model, while we also have studied critical steps of the proposed reaction pathways for more realistic vinyl-Bpin(OAc)$^-$ borate (see below). In addition, we wish to emphasize that our calculations show that the formation of the vinyl (or aryl) borate with hydroxide anion is a thermodynamically more favorable process (see Scheme S2 in Supporting Information for details).

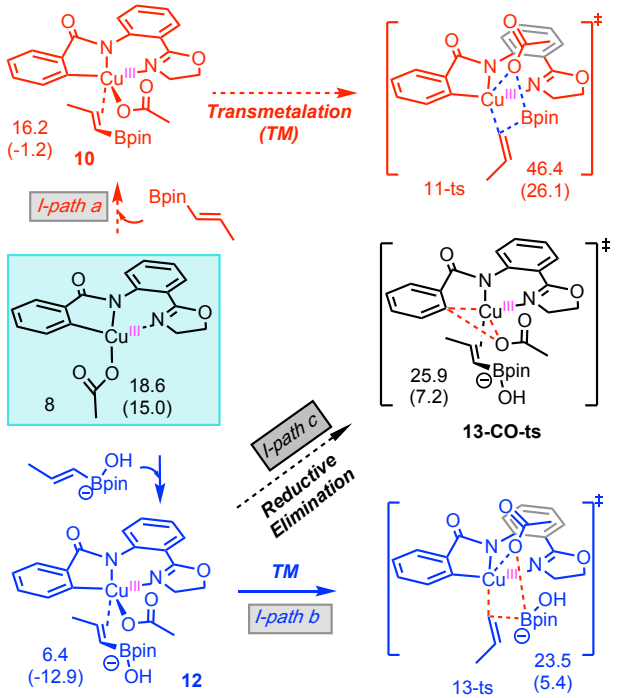

Figure 2. Pre-reaction complexes and transition states of the key mechanistic pathways (I-*path-a*, I-*path-b* and I-*path-c)* of the Type-I reactions. Relative energies of these structures are presented as ΔG(ΔH) in kcal/mol, relative to 2$Cu(OAc)_2$ + BAO + Z, where Z = vinyl-Bpin and vinyl-Bpin(OH)$^-$, for pathways I-*path-a*, and I-*path-b* and I-*path-c,* respectively.

Thus, we turned our attention to the mechanism of the reaction of Cu(III) species **8** with vinyl-Bpin(OH)$^-$ anion. This reaction may proceed via pathways I-*path-b* or I-*path-c* (Figure 2), initial step of which (i.e., the coordination of borate to complex **8**) is exergonic by 12.2 kcal/mol and leads to formation of adduct **12**. The transmetalation (I-*path-b*) from **12** occurs with 16.9 or 23.5 kcal/mol free energy barriers calculated relative to pre-reaction complex **12** or reactants (2$Cu(OAc)_2$ + BAO **+** vinyl-Bpin(OH)$^-$), respectively, at the transition state **13-ts**. The competing C–O reductive elimination (i.e., I-*path-c*) requires only 2.4 kcal/mol larger free energy barrier at the transition state **13-CO-ts**. This finding indicates that pathways I-*path-b* and I-*path-c* could effectively compete. This conclusion of computation is consistent with available experiments where the hydroxylation product was observed as a side product.[31]

Comparison of energies of the above mentioned transmetalation steps – of the charge neutral vinyl boronic ester (I-*path-a*, Figure 2) and anionic borate (vinyl-Bpin(OH)$^-$ anion, I-*path-b,* Figure 2) – shows that the pathway I-*path-b* is more favorable. This is likely due to the fact that the quaternization of the boron center with an anion (in this case, with OH^- anion) increases the nucleophilicity of the vinyl group and accelerates its transfer to the Cu(III)-center. As mentioned above, here we also validated the vinyl-Bpin(OAc)$^-$ as a model of the borate species (see Figure S2 in the Supporting Information, I-*path-d*). Briefly, we found that transmetallation with vinyl-Bpin(OAc)$^-$ occurs via a 7.2 kcal/mol higher energy barrier than that with vinyl-Bpin(OH)$^-$ (I-*path-b*).

Noteworthy, we also have explored reaction of the Cu(II) intermidate **7** with borate (see Figure S3 in the Supporting Information, I-*path-f*) and found that this reaction pathway is kinetically and thermodynamically less favorable than the above reported pathway I-*path-b* that involves the anionic borate and Cu(III) complex **8**. Therefore, here we will not discuss this pathway in detail. We explain this finding by the stronger interaction between the high-valent Cu(III) center and carbon nucleophile (in I-*path-b*) compared to the low-valent Cu(II) species with the nucleophile. It should be noted that previously Wang and coworkers have reported a similar transmetalation pathway (involving anioinc borate species and Cu(II)-intermedate) for the Cu(II)-catalyzed cross-coupling between the azacalix[1]arene[3]pyridine and aryl-boronic acid, and shown it to be the most favorable mechanism of the reaction.[51]

Overall, above presented extensive calculations have enabled us to conclude that the most favorable transmetalation in the $Cu(OAc)_2$-catalyzed BAO C(sp^2)–H bond vinylation by vinyl–Bpin starts by coordination of the *in situ* generated anionic borate to the Cu(III) intermediate **8,** and proceeds via the I-*path-b* (Figure 2) and the transition state **13-ts**. The calculated activation barrier for this pathway, 23.5 kcal/mol, is lower than that for the C–H bond activation (30.9 kcal/mol, Figure 1), which allows us to identify the C–H bond activation as a rate-limiting step of the $Cu(OAc)_2$-catalyzed BAO C(sp^2)–H bond vinylation by vinyl–Bpin. This finding is consistent with the

previous kinetic isotope effect studies.[25,31] Furthermore, the performed KIE calculations also support this conclusion. Indeed, the KIE is calculated to be 4.4 for the C-H bond activation step. This calculated KIE value is in good agreement with the experimentally reported 4.3 (for reaction 2 in Scheme 1)[26] and 3.5 (for reaction 7 in Scheme 1).[31]

3.2. The Following Steps of the $Cu(OAc)_2$-catalyzed BAO $C(sp^2)$–H Bond Vinylation by Borate after Transmetalation.

Intriguingly, the IRC calculations, initiated from the most favorable transmetalation transition state **13-ts**, led to the direct C-C coupling product **14** (Figure 3). This finding enabled us to identify the transmetalation and reductive elimination as a "concerted" process. In the resulting complex **14**, the formation of which is highly exergonic, the Cu(III) is reduced to Cu(I). The release of the H-bonded Bpin–OH fragment from intermediate **14** to generate complex **15** is slightly (by 8.6 kcal/mol) endergonic. Finally, the protodemetalation by acetic acid leads to the C–H bond vinylated product and $Cu^{I}(OAc)_2$ anion, which, then, will be oxidized by the silver salt to recover the Cu(II) catalyst.

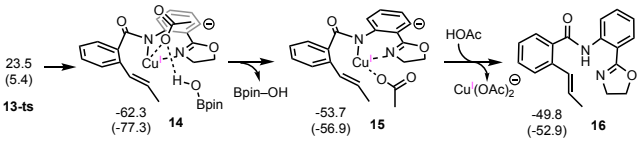

Figure 3. The following steps of the $Cu(OAc)_2$-catalyzed BAO $C(sp^2)$–H bond vinylation by borate after transmetalation.

In summary, above presented data clearly show that in the $Cu(OAc)_2$-catalyzed BAO $C(sp^2)$–H bond vinylation by vinyl–Bpin, the coupling partner is the *in situ* generated anionic borate. This reaction starts by the substrate coordination to form **2**, followed by the (a) N-H and C-H bonds activation leading to the intermediate **7**, (b) the Cu(II)/Cu(II) → Cu(I)/Cu(III) disproportionation to form low-spin Cu(III) complex **8**, (c) *in situ* generated anionic borate coordination to **8** and transmetalation to form a new C-C bond, and (d) protodemetalation to provide the final product and Cu(I) species which later oxidizes to the active catalyst. The rate-determining step of this reaction is the C–H bond activation.

Table 2. The Calculated Free Energy Barriers (in kcal/mol) for the Key Pathways of the Studied Type-I Reactions.[a)]

Coupling Partner	I-*path-a*	I-*path-b*	I-*path-c*	I-*path-f*
Vynyl-Bpin	46.4	**23.5**	25.9	26.4
Phenyl-Bpin	52.6	**28.8**	31.4	30.8

a) The barriers of the most favorable pathways are given in bold.

As mentioned above, we have also analyzed mechanism and controlling factors of another Type-I reaction given in Scheme 1, which is the C–H bond phenylation by phenyl-Bpin (all calculated data are presented in the Supporting Information). In Table 2 we summarized the calculated free energy barriers for key pathways, namely, I-*path-a* (with neutral coupling partner), I-*path-b* (energetically most favorable one, with the anionic R–$BpinOH^-$), I-*path-c* (with the anionic R–$BpinOH^-$), and I-*path-f* (that is initiated from **7** by addition of the anionic R–$BpinOH^-$) of the studied Type-I C-H vinylation and phenylation reactions. As shown in this Table, above made conclusions for the C–H vinylation are fully valid also for the reported C–H bond phenylation reaction (2) (see Scheme 1). Namely, the transmetalation with the neutral boronic esters (I-*path-a*) occurs with the highest energy barrier. On the other hand, the transmetalation with the anionic borate species (I-*path-b*) requires less energy barrier and is a most favorable one among all the studied pathways. These findings enable us to state, once again, that in the reported $Cu(OAc)_2$-catalyzed BAO $C(sp^2)$–H bond vinylation and phenylation by vinyl–Bpin and phenyl-Bpin, the coupling partners are the *in situ* generated anionic borates. Furthermore, in both reactions, the C–H activation step is the rate-determining step of overall reaction.

4. Type-II Reactions

In all Type II reactions given in Scheme 1 (i.e., reactions 4-7) the coupling partners bear acidic hydrogen, which can be deprotonated under the reaction conditions. To validate this hypothesis, we have calculated the thermodynamics of the associated acid-base reactions involving the used coupling partners in reactions 4-7 (see Scheme S3 in the Supporting Information for details). It is found that deprotonation of the participating coupling partners in reactions 4-7 are endergonic at the room temperature, 1 atm, and in DMSO. However, their anionic forms can be accessible under the used reaction conditions (i.e., 60-90 °C, and 4 h-12 h). Therefore, in our computational analyses of the mechanisms of reactions 4-7, we use both the neutral and deprotonated forms of the participating coupling partners.

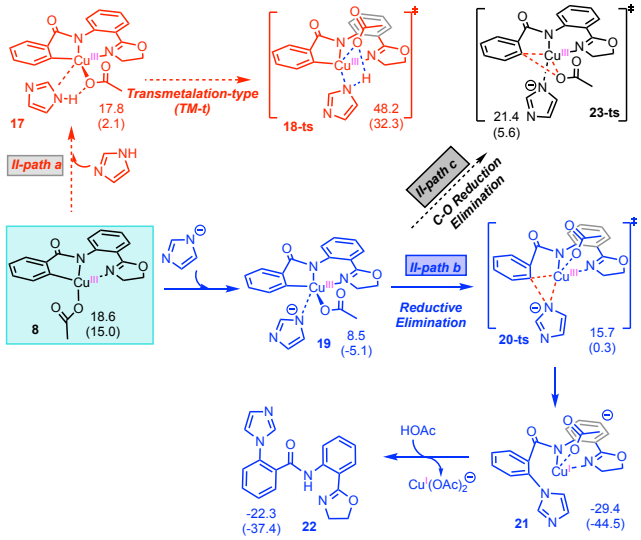

Figure 4. Reaction pathways leading to the C–H amination with imidazole from intermediate **8**.

For sake of simplicity of presenting our findings, below we use the Cu(II)-catalyzed BAO C–H bond amination by imidazole, i.e. reaction (4) (see Scheme 1), as an example. One should mention that the imidazole motif is widely present in pharmaceutical applications.[73] Since the initial steps of the Type-I and Type-II reactions (i.e., the substrate coordination, the N-H

bond activation, C-H bond deprotonation, and disproportionation steps) are same and were discussed in the Section 2, below, we start our analyses directly from the reactions of the coupling partners with intermediates **7** (before the disproportionation) and **8** (after the disproportionation).

Calculations show that the transmetalation and reductive elimination initiated directly from intermediate **7** are unfavorable (see Figure S4 in Supporting Information for details). Therefore, we start our discussion of the reaction of complex **8** with of the neutral and deprotonated forms of the participating coupling partners.

As seen in Figure 4, the coordination of neutral imidazole molecule to complex **8** is slightly (by 0.8 kcal/mol) exergonic (see structure **17**), however, the following transmetalation via the energetically lowest transition state **18-ts** requires a high free energy barrier (48.2 kcal/mol, calculated relative to the $2Cu(OAc)_2$ + BAO **+** imidazole). This finding makes the reaction of **8** and the neutral imidazole molecule (i.e., II-*path-a* in Figure 4) an unlikely process. We explain this finding by the weak basicity of the metal-bound acetate in the transmetalation process.

In contrast, the coordination of imidazole-anion to Cu(III) center of **8** to form intermediate **19**, is exergonic by 10.1 kcal/mol (Figure 4), and the following reductive elimination (II-*path-b*) to form intermediate **21** with the C-N bond requires a relatively lower energy barrier of 7.2 or 15.7 kcal/mol with respect to pre-reaction complex **19** or reactants $2Cu(OAc)_2$ + BAO **+** imidazole-anion, at the transition state **20-ts**. This step of the reaction is highly exergonic (by 48.0 or 29.4 kcal/mol, relative to reactants **8** + imidazole-anion or $2Cu(OAc)_2$ + BAO **+** imidazole-anion, respectively). The following protodemetalation (which is endergonic only by 7.1 kcal/mol) releases the amination product (**22**) and Cu(I) species. Later, Cu(I) species would be oxidized by O_2 from air to Cu(II) catalyst.

The competing C-O bond formation in intermediate **19** (i.e., II-*path-c*, Figure 4) requires 12.9 kcal/mol free energy barrier at the transition state **23-ts** (with respect to **19**). Since this energy barrier is 5.7 kcal/mol higher compared to that for the C-N reductive elimination (II-*path-b*), the formation of the C–O bond during of this reaction seems to be unlikely. Our result is consistent with experiment in which no C-O bond formation product was observed.[30] Another pathway, initiated by the ligand exchange between imidazole anion and acetate in **8**, and followed by C–N reductive elimination is found to be unfavorable (II-*path-d*, see Figure S4 in Supporting Information for details).

In summary, above presented data clearly show that in the $Cu(OAc)_2$-catalyzed BAO C(sp^2)–H amination by imidazole, the real coupling partner is the *in situ* generated imidazole anion via deprotonation by the base. This reaction, like the above discussed Type-I reactions, starts from the substrate coordination to $Cu(OAc)_2$, the N-H and C-H bonds activation, and disproportionation steps leading to formation of low-spin Cu(III) complex **8**, and follows by the coordination of the *in situ* generated imidazole anion (via deprotonation by the base) to **8**, the C-N bond reductive elimination, protodemetalation, and catalyst re-generation via oxidation of Cu(I) species by O_2 molecule. The rate-determining step of this reaction, same as in the Type-I reactions, is the C–H bond activation.

As mentioned above we also have studied other Type-II reactions including the C–H bond amination with aromatic amines, alkynylation with phenyl-substituted terminal alkyne, and hydroxylation with water (see reactions (5-7) in Scheme 1). All calculated data are presented in the Supporting Information (see Figures S5-S7). In Table 3 we summarized the calculated free energy barriers for key pathways, namely, II-*path-a* (with neutral coupling partner), II-*path-b* (with the anionic coupling partner), II-*path-c* (with the anionic coupling partner), and II-*path-f*, (also, with anionic coupling partner, by with complex **7**) of the studied Type-II reactions. As seen from this Table, above made conclusions for the C–H amination with imidazole are also valid for other Type-II reactions (see Scheme 1, eqs. 5-7).

Table 3. The Calculated Free Energy Barriers (in kcal/mol) for the Key Pathways of the Studied Type-II Reactions.[a,b]

Coupling Partner	**II-***path-a*	**II-***path-b*	**II-***path-c*	**II-***path-f*
Imidazole	48.2	**15.7**	21.4	43.7
Aniline	27.8	**2.7**	19.9	37.3
Phenylacetylene	50.3	**1.2**	13.9	23.1
Water	33.8	**6.2**	15.3	33.7

a) The barriers of the most favorable pathways are given in bold.
b) The acid-base equilibria is not included in the given energies.

Indeed, the neutral transmetalation pathways (II-*path-a*) for all studied reactions are highly unfavorable. The II-*path-b* pathway which starts by the coordination of the deprotonated coupling partner to Cu(III) complex **8** and followed by the C–X reductive elimination is the most favorable one, for all studied reactions. In addition, the C-O reductive elimination (II-*path-c*) occurs with at least 5.7 kcal/mol more energy barrier than II-*path-b*, which makes it unfavorable for all studied Type-II reactions.

5. Special Case: the $Cu(OAc)_2$-catalyzed C(sp^2)–H Trifluoromethylation with $TMSCF_3$.

Our extensive calculations of the mechanism of the reported Cu(II)-catalyzed BAO C(sp^2)–H bond trifluoromethylation with $TMSCF_3$ enabled us to identify it as a special case, that is positioned between the Type–I and Type–II reaction types. Indeed, we find that the transmetalation with a neutral $TMSCF_3$ requires a free energy barrier of 68.1 kcal/mol and is not feasible (see Figure S8 in the Supporting Information). Meanwhile, treating it as a Type-I reaction and adding OH^- (or AcO^-) to the silicon center led to dissociation of the CF_3^- anion. In other words, in the basic reaction conditions $TMSCF_3$ is expected to undergo ligand exchange between the OH^- (or AcO^-) and CF_3^- anion (this ligand exchange reaction is exergonic by 32.3 kcal/mol, see Scheme S4 in the Supporting Information). The generated CF_3^- anion readily binds to the electrophilic Cu(III) center of **8** and undergoes the C–C reductive elimination, like in other above reported Type-II reactions. The presented calculations show that the binding of the CF_3^- anion to the copper center of **8** is exergonic by 31.6 kcal/mol and the subsequent C–C reductive elimination occurs only with a 2.1 kcal/mol free energy barrier (see Figure S8 in the Supporting Information). Thus, in the reported Cu(II)-catalyzed C(sp^2)–H bond trifluoromethylation with $TMSCF_3$, the real coupling partner is the *in situ* generated (via the CF_3^--to-OH^- (or AcO^-) ligand exchange)

CF_3^- anion (like in the Type-I reactions) that binds to the Cu(III)-center of intermediate **8**, and promotes the C–CF_3 reductive elimination (like in the Type-II reactions).

Conclusion

In summary, we have performed comprehensive studies of the mechanisms of seven Cu(II)-catalyzed and oxazoline (Oxa) ligand directed benzamide-oxazoline, BAO, C(sp^2)–H bond functionalization reactions, such as (see the reactions 1-7 in Scheme 1) vinylation and phenylation, trifluoromethylation, amination, alkynylation, and hydroxylation. We found that (see Scheme 4):

(a) initial steps of these reactions are the directing-group assisted substrate coordination to the Cu(II)-center, N–H and C–H bond deprotonation leading to formation of intermediate **7** (or **B'** in Scheme 4), and the Cu(II)/Cu(II) → Cu(I)/Cu(III) disproportionation to form Cu(III) intermediate **8** (or **C** in Scheme 4). This overall process (i.e., the intermediate **C** formation) is endergonic by 18.6 kcal/mol and requires maximum of 30.9 kcal/mol free energy barrier for the C–H bond activation. The mechanisms these reactions are diverging from the intermediate **C** and are strongly dependent on the true nature of the participating coupling partners under the reaction conditions.

(b) the realistic coupling partners in the C(sp^2)–H bond vinylation and phenylation with vinyl or phenyl boronic esters (R–Bpin), respectively, are the corresponding *in situ* generated anionic borates. From intermediate **C,** these reactions, labeled as a Type-I reactions where original coupling partners have no acidic hydrogen atom, proceed via the (a) anionic borate coordination to the Cu(III)-center, (b) concerted transmetalation and reductive elimination, and (c) protodemetalation steps (Scheme 4, blue). The vinyl and phenyl borates transmetalation have a barrier of 23.5 and 28.8 kcal/mol, respectively. These barriers are by 2.4 and 2.6 kcal/mol, respectively, smaller than that for the competing direct C-O reductive elimination, which is consistent with experiments reporting only minor C–O formation product.

(c) in the Type-II reactions, where original coupling partners bear acidic hydrogen atoms (like imidazole, $ArNH_2$, terminal alkyne, and H_2O), the realistic coupling partners are the *in situ* generated deprotonated species. From intermediate **C**, these reactions follow via the (a) coordination of deprotonated coupling partners to the Cu(III)-center, and (b) C-Y (where, Y = C, N and O) reductive elimination steps (Scheme 4, in red).

(d) The reported C(sp^2)–H trifluoromethylation with $TMSCF_3$ is a special case: it is positioned between the Type-I and Type–II reaction types, because of labile nature of the Si–CF_3 bond. Indeed, this reaction starts by the OH^- (or AcO^-) addition to $TMSCF_3$ (like in the Type-I reactions), proceeds via the CF_3^--to-OH^- (or AcO^-) exchange, and the C–CF_3 reductive elimination (like in the Type-II reactions) steps (Scheme 4, in red).

(e) the rate-determining step of all studied reactions is the C-H bond activation step, which is consistent with the reported kinetic isotope effects.[25,31]

Scheme 4. A Unified Mechanism for the Cu(II)-Catalyzed/Mediated and Oxa-Directed C(sp^2)-H Functionalization.

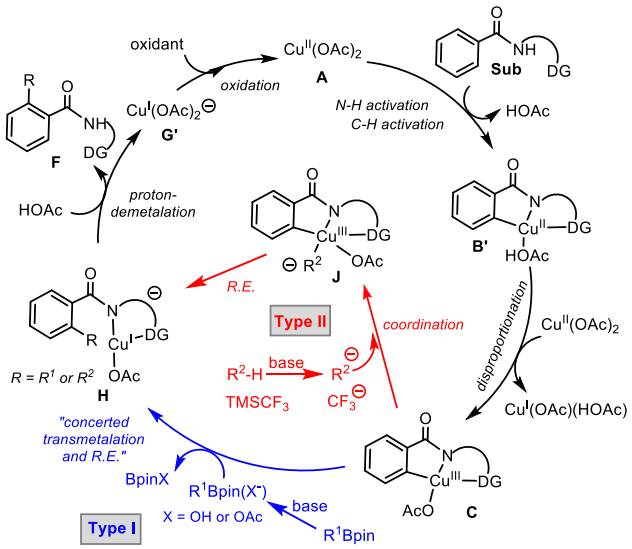

ASSOCIATED CONTENT

Supporting Information

Computational details, energies and frequency analysis, Cartesian coordinates of all reported structures. Figures S1–S11 and Schemes S1–S4. This material is available free of charge via the Internet at http://pubs.acs.org.

AUTHOR INFORMATION

Corresponding Author

*E-mail: dmusaev@emory.edu

Authors Contributions

Dr. L.-P.X. has performed most of the calculations, and has played a key role in the scientific designing of this project, and wrote the manuscript under the supervision of Dr. D.G.M.; Dr. B.E.H. has performed calculations of most structures and TSs associated with the C–H bond activation step, and contributed to the project discussion and manuscript preparation; Dr. M.J.A. has performed part of calculations of structures related to the C–H bond activation step; Dr. J.-Q.Y. has proposed the studied reactions and has contributed to the manuscript preparation, and Dr. D.G.M. has supervised all the presented calculations, project designing, and manuscript preparation.

Notes

The authors declare no competing financial interests.

ACKNOWLEDGMENT

This work was supported by the National Science Foundation under the CCI Center for Selective C–H Functionalization (CHE-1700982). The authors gratefully acknowledge the use of the resources of the Cherry Emerson Center for Scientific Computation at Emory University. L.-P. Xu acknowledges the Natural Science Foundation of China (NSFC 21702126) and the China Scholarship Council for support.

REFERENCES

1. Kakiuchi, F.; Sekine, S.; Tanaka, Y.; Kamatani, A.; Sonoda, M.; Chatani, N.; Murai, S., Catalytic Addition of Aromatic Carbon–

Hydrogen Bonds to Olefins with the Aid of Ruthenium Complexes. *Bull. Chem. Soc. Jpn.* **1995**, *68*, 62-83.

2. Chen, X.; Engle, K. M.; Wang, D.-H.; Yu, J.-Q., Palladium(II)-Catalyzed C-H Activation/C-C Cross-Coupling Reactions: Versatility and Practicality. *Angew. Chem. Int. Ed.* **2009**, *48*, 5094-5115.

3. Giri, R.; Shi, B.-F.; Engle, K. M.; Maugel, N.; Yu, J.-Q., Transition Metal-catalyzed C–H Activation Reactions: Diastereoselectivity and Enantioselectivity. *Chem. Soc. Rev.* **2009**, *38*, 3242-3272.

4. Colby, D. A.; Bergman, R. G.; Ellman, J. A., Rhodium-Catalyzed C–C Bond Formation via Heteroatom-Directed C−H Bond Activation. *Chem. Rev.* **2010**, *110*, 624-655.

5. Lyons, T. W.; Sanford, M. S., Palladium-Catalyzed Ligand-Directed C−H Functionalization Reactions. *Chem. Rev.* **2010**, *110*, 1147-1169.

6. Wencel-Delord, J.; Dröge, T.; Liu, F.; Glorius, F., Towards Mild Metal-catalyzed C–H Bond Activation. *Chem. Soc. Rev.* **2011**, *40*, 4740-4761.

7. Arockiam, P. B.; Bruneau, C.; Dixneuf, P. H., Ruthenium(II)-Catalyzed C–H Bond Activation and Functionalization. *Chem. Rev.* **2012**, *112*, 5879-5918.

8. Ackermann, L., Carboxylate-Assisted Ruthenium-Catalyzed Alkyne Annulations by C–H/Het–H Bond Functionalizations. *Acc. Chem. Res.* **2014**, *47*, 281-295.

9. Gandeepan, P.; Muller, T.; Zell, D.; Cera, G.; Warratz, S.; Ackermann, L., 3d Transition Metals for C-H Activation. *Chem. Rev.* **2019**, *119*, 2192-2452.

10. Shang, R.; Ilies, L.; Nakamura, E., Iron-Catalyzed C–H Bond Activation. *Chem. Rev.* **2017**, *117*, 9086-9139.

11. Varela-Álvarez, A.; Musaev, D. G., Can the bis(imino)pyridine Iron, (PDI)FeL^1L^2, Complex Catalyze C-H Bond Functionalization?, *Chem Sci.,* **2013**, *4*, 3758-3764.

12. Moselage, M.; Li, J.; Ackermann, L., Cobalt-Catalyzed C–H Activation. *ACS Catal.* **2016**, *6*, 498-525.

13. Xu, L.-P.; Liu, E. E. L.-N.; Bacsa, J.; MacBeth, C. E.; Musaev, D. G., Mechanistic Details of the Cobalt-Mediated Dehydrogenative Dimerization of Aminoquinoline-Directed Benzamides, *Chem Sci*., **2020**, *11*, 6085-6096.

14. Aihara, Y.; Chatani, N., Nickel-Catalyzed Direct Arylation of C(sp3)–H Bonds in Aliphatic Amides via Bidentate-Chelation Assistance. *J. Am. Chem. Soc.* **2014**, *136*, 898-901.

15. Yamaguchi, J.; Muto, K.; Itami, K., Nickel-Catalyzed Aromatic C-H Functionalization. *Top. Curr. Chem*. **2016**, *374*, 55.

16. Xu, H.; Muto, K.; Yamaguchi, J.; Zhao, C.; Itami, K.; Musaev, D. G., Key Mechanistic Features of Ni-catalyzed C–H/C–O Biaryl Coupling of Azoles and Naphthalen-2-yl Pivalates, *J. Am. Chem. Soc.* **2014**, *136*, 14834-14844.

17. Guo, X.-X.; Gu, D.-W.; Wu, Z.; Zhang, W., Copper-Catalyzed C–H Functionalization Reactions: Efficient Synthesis of Heterocycles. *Chem. Rev.* **2015**, *115*, 1622-1651.

18. Rao, W.-H.; Shi, B.-F., Recent Advances in Copper-Mediated Chelation-assisted Functionalization of Unactivated C–H Bonds. *Org. Chem. Front.* **2016**, *3*, 1028-1047.

19. Haines, B. E.; Kawakami, T.; Murakami, K.; Itami, K.; Musaev, D. G., Key Mechanistic Details and predictive Models for Cu-catalyzed Aromatic C-H Imidation with *N*-Fluorobenzenesulfonimide. *Chem. Sci.,* **2017**, *8*, 988-1002.

20. Davies, H. M. L.; Morton, D., Recent Advances in C–H Functionalization. *J. Org. Chem.* **2016**, *81*, 343-350.

21. Kulkarni, A. A.; Daugulis, O., Direct Conversion of Carbon-Hydrogen into Carbon-Carbon Bonds by First-Row Transition-Metal Catalysis. *Synthesis* **2009**, *2009*, 4087-4109.

22. Su, B.; Cao, Z.-C.; Shi, Z.-J., Exploration of Earth-Abundant Transition Metals (Fe, Co, and Ni) as Catalysts in Unreactive Chemical Bond Activations. *Acc. Chem. Res.* **2015**, *48*, 886-896.

23. Chen, X.; Hao, X.-S.; Goodhue, C. E.; Yu, J.-Q., Cu(II)-Catalyzed Functionalizations of Aryl C–H Bonds Using O_2 as an Oxidant. *J. Am. Chem. Soc.* **2006**, *128*, 6790-6791.

24. Trammell, R.; Rajabimoghadam, K.; Garcia-Bosch, I., Copper-Promoted Functionalization of Organic Molecules: from Biologically Relevant Cu/O_2 Model Systems to Organometallic Transformations. *Chem. Rev.* **2019**, *119*, 2954-3031.

25. Li, J. J.; Wang, C. G.; Yu, J. F.; Wang, P.; Yu, J. Q., Cu-Catalyzed C-H Alkenylation of Benzoic Acid and Acrylic Acid Derivatives with Vinyl Boronates. *Org. Lett.* **2020**, *22*, 4692-4696.

26. Shang, M.; Sun, S. Z.; Dai, H. X.; Yu, J. Q., $Cu(OAc)_2$-catalyzed Coupling of Aromatic C-H bonds with Arylboron Reagents. *Org. Lett*. **2014**, *16*, 5666-5669.

27. Shang, M.; Sun, S.-Z.; Wang, H.-L.; Laforteza, B. N.; Dai, H.-X.; Yu, J.-Q., Exceedingly Fast Copper(II)-Promoted ortho C-H Trifluoromethylation of Arenes using $TMSCF_3$. *Angew. Chem. Int. Ed.* **2014**, *53*, 10439-10442.

28. Yu, J.-F.; Li, J.-J.; Wang, P.; Yu, J.-Q., Cu-Mediated Amination of (Hetero)Aryl C−H bonds with NH Azaheterocycles. *Angew. Chem. Int. Ed.* **2019**, *58*, 18141-18145.

29. Shang, M.; Sun, S. Z.; Dai, H. X.; Yu, J. Q., Cu(II)-mediated C-H Amidation and Amination of Arenes: Exceptional Compatibility with Heterocycles. *J. Am. Chem. Soc.* **2014**, *136*, 3354-3557.

30. Shang, M.; Wang, H. L.; Sun, S. Z.; Dai, H. X.; Yu, J. Q., Cu(II)-mediated ortho C-H Alkynylation of (Hetero)Arenes with Terminal Alkynes. *J. Am. Chem. Soc.* **2014**, *136*, 11590-11593.

31. Sun, S.-Z.; Shang, M.; Wang, H.-L.; Lin, H.-X.; Dai, H.-X.; Yu, J.-Q., Cu(II)-Mediated C(sp^2)–H Hydroxylation. *J. Org. Chem.* **2015**, *80*, 8843-8848.

32. Yang, Y.-F.; Hong, X.; Yu, J.-Q.; Houk, K. N., Experimental–Computational Synergy for Selective Pd(II)-Catalyzed C–H Activation of Aryl and Alkyl Groups. *Acc. Chem. Res.* **2017**, *50*, 2853-2860.

33. Musaev, D. G.; Figg, T. M.; Kaledin, A. L., Versatile Reactivity of Pd-catalysts: Mechanistic Features of the Mono-N-protected Amino Acid Ligand and Cesium-halide Base in Pd-catalyzed C–H Bond Functionalization. *Chem. Soc. Rev.* **2014**, *43*, 5009-5031.

34. Engle K. M., The Mechanism of Palladium (II)-Mediated C–H Cleavage with Mono-N-Protected Amino Acid (MPAA) Ligands: Origins of Rate Acceleration. *Pure. Appl. Chem.* **2016**, *88*, 119-138.

35. Musaev, D. G.; Kaledin, A.; Shi, B.-F.; Yu, J.-Q., Key Mechanistic Features of Enantioselective C-H Bond Activation Reactions Catalyzed by [(Chiral Mono-N-Protected Amino Acid)-Pd(II)] Complexes. *J. Am. Chem. Soc.* **2012**, *134*, 1690-1698.

36. Figg, T. M.; Wasa, M.; Yu, J.-Q.; Musaev, D. G., Understanding the Reactivity of Pd(0)/PR_3 Catalyzed Intermolecular C(sp^3)-H bond Arylation. *J. Am. Chem. Soc.* **2013**, *135*, 14206-14214.

37. Yang, Y.-F.; Cheng, G.-J.; Liu, P.; Leow, D.; Sun, T.-Y.; Chen, P.; Zhang, X.; Yu, J.-Q.; Wu, Y.-D.; Houk, K. N., Palladium-Catalyzed Meta-Selective C–H Bond Activation with a Nitrile-Containing Template: Computational Study on Mechanism and Origins of Selectivity. *J. Am. Chem. Soc.* **2014**, *136*, 344-355.

38. Cheng, G.-J.; Yang, Y.-F.; Liu, P.; Chen, P.; Sun, T.-Y.; Li, G.; Zhang, X.; Houk, K. N.; Yu, J.-Q.; Wu, Y.-D., Role of N-Acyl Amino Acid Ligands in Pd(II)-Catalyzed Remote C–H Activation of Tethered Arenes. *J. Am. Chem. Soc.* **2014**, *136*, 894-897.

39. Haines, B. E.; Xu, H.; Verma, P.; Wang, X.; Yu, J.-Q.; Musaev, D. G., Mechanistic Details of Pd(II)-Catalyzed C-H Iodination with Molecular I_2: Oxidative Addition *vs* Electrophilic Cleavage. *J. Am. Chem. Soc.* **2015**, *137*, 9022-9031.

40. Haines, B. E.; Yu, J.-Q.; Musaev, D. G., Enantioselectivity Model for Pd-Catalyzed C–H Functionalization Mediated by the Mono-N-Protected Amino Acid (MPAA) Family of Ligands. *ACS Catal.* **2017**, *7*, 4344-4354.

41. Haines, B. E.; Berry, J. F.; Yu, J.-Q.; Musaev, D. G., Factors Controlling Stability and Reactivity of Dimeric Pd (II)-Complexes in C–H Functionalization Catalysis. *ACS Catal.* **2016**, *6*, 829-839.

42. Chen, G.; Gong, W.; Zhuang, Z.; Andra, M. S.; Chen, Y.-Q.; Hong, X.; Yang, Y.-F.; Liu, T.; Houk, K. N.; Yu, J.-Q., Ligand-Accelerated Enantioselective Methylene C(sp^3)-H Bond Activation. *Science*. **2016**, *353*, 1023-1027.

43. Weingarten, A. Copper comeuppance. *Nat. Rev. Chem.* **2020**, *4*, 3.

44. DiMucci, I. M.; Lukens, J. T.; Chatterjee, S.; Carsch, K. M.; Titus, C. J.; Lee, S. J.; Nordlund, D.; Betley, T. A.; MacMillan, S. N.; Lancaster, K. M., The myth of d^8 Copper(III), *J. Am. Chem. Soc.* **2011**, *133*, 7668-7671.

45. Wendlandt, A. E.; Suess, A. M.; Stahl, S. S., Copper-Catalyzed Aerobic Oxidative C-H Functionalizations: Trends and Mechanistic Insights. *Angew. Chem. Int. Ed.* **2011**, *50*, 11062-11087.

46. Chen, B.; Hou, X.-L.; Li, Y.-X.; Wu, Y.-D., Mechanistic Understanding of the Unexpected Meta Selectivity in Copper-Catalyzed Anilide C–H Bond Arylation *J. Am. Chem. Soc.* **2011**, *133*, 7668-7671.

47. Hamada, T.; Ye, X.; Stahl, S. S., Copper-Catalyzed Aerobic Oxidative Amidation of Terminal Alkynes: Efficient Synthesis of Ynamides. *J. Am. Chem. Soc.* **2008**, *130*, 833-835.

48. Monguchi, D.; Fujiwara, T.; Furukawa, H.; Mori, A., Direct Amination of Azoles via Catalytic C−H, N−H Coupling. *Org. Lett.* **2009**, *11*, 1607-1610.

49. Banerjee, A.; Santra, S. K.; Rout, S. K.; Patel, B. K., A Ligand Free Copper(II) Catalyst Is as Effective as A Ligand Assisted Pd(II) Catalyst towards Intramolecular C–S Bond Formation via C–H Functionalization. *Tetrahedron* **2013**, *69*, 9096-9104.

50. Suess, A. M.; Ertem, M. Z.; Cramer, C. J.; Stahl, S. S., Divergence between Organometallic and Single-Electron-Transfer Mechanisms in Copper(II)-Mediated Aerobic C–H Oxidation. *J. Am. Chem. Soc.* **2013**, *135*, 9797-9804.

51. Zhang, Q.; Liu, Y.; Wang, T.; Zhang, X.; Long, C.; Wu, Y.-D.; Wang, M.-X., Mechanistic Study on Cu(II)-Catalyzed Oxidative Cross-Coupling Reaction between Arenes and Boronic Acids under Aerobic Conditions. *J. Am. Chem. Soc.* **2018**, *140*, 5579-5587

52. Hall, D. G. Structure, Properties, and Preparation of Boronic Acid Derivatives. *Wiley-VCH:* **2011**, pp 9-12.

53. Lorand, J. P.; Edwards, J. O., Polyol Complexes and Structure of the Benzeneboronate Ion. *J. Org. Chem.* **1959**, *24*, 769-774.

54. Cammidge, A. N.; Goddard, V. H. M.; Gopee, H.; Harrison, N. L.; Hughes, D. L.; Schubert, C. J.; Sutton, B. M.; Watts, G. L.; Whitehead, A. J., Aryl Trihydroxyborates: Easily Isolated Discrete Species Convenient for Direct Application in Coupling Reactions. *Org. Lett.* **2006**, *8*, 4071-4074.

55. Carrow, B. P.; Hartwig, J. F., Distinguishing Between Pathways for Transmetalation in Suzuki−Miyaura Reactions. *J. Am. Chem. Soc.* **2011**, *133*, 2116-2119.

56. Thomas, A. A.; Denmark, S. E., Pre-transmetalation Intermediates in the Suzuki-Miyaura Reaction Revealed: The Missing Link. *Science* **2016**, *352*, 329-332.

57. Das, A.; Ren, Y.; Hessin C.; Murr, M. D-E., Copper Catalysis with Redox-Active Ligands. *Beilstein J. Org. Chem.* **2020**, *16*, 858-870.

58. Lim, H.; Thomas, K. E.; Hedman, B.; Hodgson, K. O.; Ghosh, A.; Solomon, E. I. X-ray Absorption Spectroscopy as a Probe of Ligand Noninnocence in Metallocorroles: The Case of Copper Corroles. Inorg. Chem.2019,58, 6722−6730.

59. Kirillov, A. M.; Kirillova, M. V.; Pombeiro, A. J. L., Multicopper complexes and coordination polymers for mild oxidative functionalization of alkanes, *Coord. Chem. Rev.* **2012**, *256*, 2741-2759.

60. Elwell, C. E.; Gagnon, N. L.; Neisen, B. D.; Dhar, D.; Spaeth, A.D.; Yee, G. M.; Tolman, W. B. Copper-Oxygf72en Complexes Revisited: Structures, Spectroscopy, and Reactivity. *Chem. Rev.* **2017**, 117, 2059−2107.

61. Frisch, M. J.; Trucks, G. W.; Schlegel, H. B.; Scuseria, G. E.; Robb, M. A.; Cheeseman, J. R.; Scalmani, G.; Barone, V.; Petersson, G. A.; Nakatsuji, H.; Li, X.; Caricato, M.; Marenich, A. V.; Bloino, J.; Janesko, B. G.; Gomperts, R.; Mennucci, B.; Hratchian, H. P.; Ortiz, J. V.; Izmaylov, A. F.; Sonnenberg, J. L.; Williams-Young, D.; Ding, F.; Lipparini, F.; Egidi, F.; Goings, J.; Peng, B.; Petrone, A.; Henderson, T.; Ranasinghe, D.; Zakrzewski, V. G.; Gao, J.; Rega, N.; Zheng, G.; Liang, W.; Hada, M.; Ehara, M.; Toyota, K.; Fukuda, R.; Hasegawa, J.; Ishida, M.; Nakajima, T.; Honda, Y.; Kitao, O.; Nakai, H.; Vreven, T.; Throssell, K.; Montgomery, J. A., Jr.; Peralta, J. E.; Ogliaro, F.; Bearpark, M. J.; Heyd, J. J.; Brothers, E. N.; Kudin, K. N.; Staroverov, V. N.; Keith, T. A.; Kobayashi, R.; Normand, J.; Raghavachari, K.; Rendell, A. P.; Burant, J. C.; Iyengar, S. S.; Tomasi, J.; Cossi, M.; Millam, J. M.; Klene, M.; Adamo, C.; Cammi, R.; Ochterski, J. W.; Martin, R. L.; Morokuma, K.; Farkas, O.; Foresman, J. B.; Fox, D. J., *Gaussian 09*, Revision D.01, Gaussian, Inc., Wallingford CT, **2015**.

62. Hay, P. J.; Wadt, W. R., Ab initio Effective Core Potentials for Molecular Calculations. Potentials for K to Au including the Outermost Core Orbitals. *J. Chem. Phys.* **1985,** *82*, 299-310.

63. Wadt, W. R.; Hay, P. J., Ab initio Effective Core Potentials for Molecular Calculations. Potentials for Main Group Elements Na to Bi. *J. Chem. Phys.* **1985,** *82*, 284-298.

64. Becke, A. D., Density-functional Exchange-energy Approximation with Correct Asymptotic Behavior. *Phys. Rev. A* **1988,** *38*, 3098-3100.

65. Lee, C.; Yang, W.; Parr, R. G., Development of the Colle-Salvetti Correlation-energy Formula into a Functional of the Electron Density. *Phys. Rev. B* **1988,** *37*, 785-789.

66. Becke, A. D., A New Mixing of Hartree–Fock and Local Density-Functional Theories. *J. Chem. Phys.* **1993,** *98*, 1372-1377.

67. Grimme, S.; Antony, J.; Ehrlich, S.; Krieg, H., A Consistent and Accurate Ab initio Parametrization of Density Functional Dispersion Correction (DFT-D) for the 94 Elements H-Pu. *J. Chem. Phys.* **2010,** *132*, 154104.

68. Grimme, S.; Hansen, A.; Brandenburg, J. G.; Bannwarth, C., Dispersion-corrected Mean-field Electronic Structure Methods. *Chem. Rev.* **2016**, *116*, 5105-5154.

69. Cancès, E.; Mennucci, B.; Tomasi, J., A New Integral Equation Formalism for the Polarizable Continuum Model: Theoretical Background and Applications to Isotropic and Anisotropic Dielectrics. *J. Chem. Phys.* **1997,** *107*, 3032-3041.

70. It should be noted that the ΔE value is higher in **3-ts** than in the product, **4**.

71. Miyaura, N.; Suzuki, A. Palladium-Catalyzed Cross-Coupling Reactions of Organoboron Compounds. *Chem. Rev.* **1995**, *95*, 2457-2483.

72. Kurti, L.; Czako, B., Strategic Applications of Named Reactions in Organic Synthesis, *Elsevier Academic Press*, **2005**, *1st Edition*, 448-449.

73. Leon Shargel., Comprehensive Pharmacy Review (7th ed.), p. 930. *ISBN 9780781765617,* **1996.**

Insert Table of Contents artwork here